Inorganic Chemistry

Article

pubs.acs.org/IC

Experimental Evidence and DFT Studies of Next-Nearest-Neighbor Magnetic Interactions through Diamagnetic 3d and 4d Ions

Jean-Pierre Costes,*[,†,‡] Carine Duhayon,[†,‡] Laure Vendier,[†,‡] Enrique Colacio,[§] Antonio J. Mota Ávila,*[,§] and Jose Suarez Varela[§]

[†]CNRS, LCC (Laboratoire de Chimie de Coordination), 205 route de Narbonne, F-31077 Toulouse, France

[‡]Université de Toulouse, UPS, INPT, LCC, F-31077 Toulouse, France

[§]Departamento de Química Inorgánica, Facultad de Ciencias, Universidad de Granada, Av. Fuentenueva s/n, 18002-Granada, Spain

Supporting Information

ABSTRACT: The copper template effect allows the preparation of tridentate ligands that chelate copper ions, leaving unoccupied the fourth basal coordination position and at least one axial position of the copper coordination polyhedron. Two such cationic complexes, $[LCu]^+$ and $[L^1Cu]^+$ (L^- = 2-{(*E*)-[(2-aminoethyl)imino]methyl}-phenoxo] and L^{1-} = 2-{(*E*)-[(2-aminopropyl)imino]methyl}-phenoxo), react with diamagnetic polycyanometalate tectons such as $Ni(CN)_4^{2-}$ or $Ag(CN)_2^-$ to yield different neutral 1D complexes. In $\{[(LCu)_2Ni(CN)_4]\}_n$ (**1**) the four cyano nitrogen atoms are involved in coordination with copper ions in such a manner that each copper atom is pentacoordinated and linked to two cyano functions that occupy axial and equatorial coordination positions. Two L^1Cu^+ cationic entities are linked, through their equatorial plane, to two trans cyano groups of the $Ni(CN)_4^{2-}$ tecton in complex $[(L^1Cu)_2Ni(CN)_4]$ (**2**), the two uncoordinated cyano groups being involved in hydrogen bonds. **2** is a racemate, a *S* stereoisomer being associated with a *R* one in each $[(L^1Cu)_2Ni(CN)_4]$ unit. Zigzag Cu−Ag chains are present in $[(LCu)Ag(CN)_2]$ (**3**), where the copper centers are pentacoordinated and connected to the cyano groups in an alternate axial−equatorial coordination scheme. A bidimensional structure is developed by interchain argentophilic interactions. In complex **4**, $\{(L^1CuMeOH)(L^1Cu)[Ag(CN)_2]_2\}$, two L^1Cu units are connected by a NC−Ag−CN bridge in an equatorial position. These resulting units exhibit argentophilic interactions with $[Ag(CN_2)]^-$ entities that are monocoordinated in the equatorial position to the next unit, ultimately leading to a chain. Weak Cu−Cu magnetic interactions are detected in the four compounds, antiferromagnetic in the case of equatorial−equatorial copper interactions, ferromagnetic for orthogonal interacting copper orbitals (axial−equatorial interactions), while axial−axial bridges are characterized by an absence of interaction. The presence of weak ferromagnetic interactions through large NC−Ni−CN or NC−Ag−CN bridges (Cu···Cu distances larger than 10 Å) furnishes experimental evidence for the existence of next-nearest-neighbor interactions through diamagnetic centers. DFT calculations do confirm the existence of these magnetic transmission pathways through the diamagnetic metal bridge.

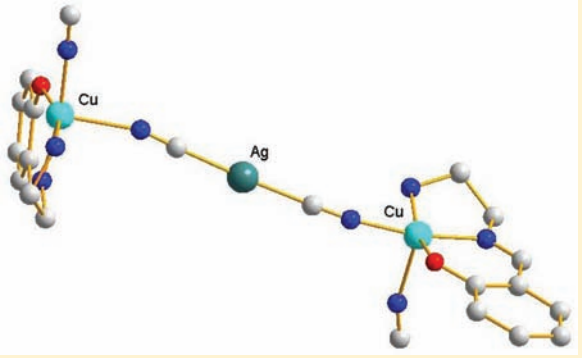

INTRODUCTION

The chemistry of polycyanometallate tectons assembling various complex cations yielded a large number of heteropolynuclear complexes during the last two decades.[1] These syntheses first used paramagnetic tectons, such as $[M(CN)_6]^{3-}$ ($M = Fe^{III}$, Cr^{III}) or $[M(CN)_8]^{3-}$ ($M = Mo^V$, W^V), and metal ions, while organic molecules with various denticities have been used to limit the number of coordination sites on the cationic metal−ligand species.[2] Of course, the chemistry of diamagnetic polycyanometallate tectons was less developed because of its limited interest in the study of magnetic properties.[3] In the past, we described methods for obtaining tridentate ligands able to react with $3d^{II}$ ions and to give complexes in which the fourth equatorial coordination site is occupied by a monodentate ligand that can be easily removed.[4] The template effect of copper has also yielded several complexes in cases where the tridentate ligands resulting from reaction of aldehyde or ketone functions with diamines are not accessible by a pure organic synthetic process.[5] The resulting copper complexes exhibit a square planar or square pyramidal environment with their d_{x2-y2} magnetic orbital localized in the basal plane. It is evident that the magnetic interaction with another metal ion will be more efficient if the bridging ligand is introduced in the basal plane of the copper complex. This is even more important in the present case where we want to evidence magnetic interactions through diamagnetic ions. As bridging ligands, we retained $[Ni(CN)_4]^{2-}$and $[Ag(CN)_2]^-$ tectons that impose formation of

Received: October 5, 2011
Published: December 23, 2011

   dx.doi.org/10.1021/ic202157q | *Inorg. Chem.* 2012, 51, 1011−1019

long NC−M−CN bridges (M = Ni^{II}, Ag^{I}) in the resulting complexes. Here, we report on the syntheses, structural determinations, magnetic properties, and DFT calculations of complexes resulting from reaction of these polycyanometallate tectons with two cationic LCu and L^1Cu species (L and L^1, see Figure 1). We will see that the use of an asymmetric ligand

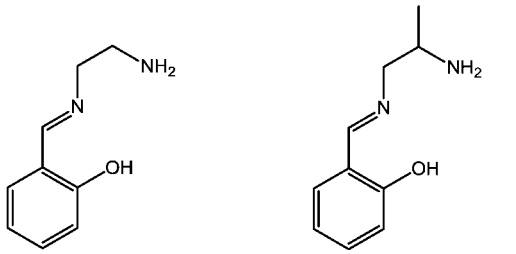

2-{(*E*)-[(2-aminoethyl)imino]methyl}phen 2-{(*E*)-[(2-aminopropyl)imino]methyl}phenol

Figure 1. Copper-chelating L (left) and L^1 (right) ligands used in this work.

under its racemate form will simplify the understanding of the magnetic interactions through diamagnetic metal ions.

EXPERIMENTAL SECTION

Materials. The starting complexes $[LCuPy](ClO_4)$[5a] and $[(LCu)_3OH](ClO_4)_2$[5b] [L = 2-{(*E*)-[(2-aminoethyl)imino]methyl}-phenoxo] were prepared as previously described. Syntheses of the L^1 ligand [L^1 = 2-{(*E*)-[(2-aminopropyl)imino]methyl}phenoxo] and its related complexes are described here. The metal salts $K_2Ni(CN)_4$ and $KAg(CN)_2$ were used as purchased. High-grade methanol (Normapur, VWR) and distilled water were used for preparing the different solutions.

Complexes. *$[L^1CuPy](ClO_4)$.* To a stirred methanol solution (50 mL) of salicylaldehyde (1.22 g, 1×10^{-2} mol) was first added copper perchlorate (3.7 g, 1×10^{-2} mol) dissolved in water (10 mL) and then pyridine (2.4 g, 3×10^{-2} mol). A few minutes later, a methanol solution of 1,2-diaminopropane (0.74 g, 1×10^{-2} mol) was added at once with stirring at room temperature. Three hours later, the precipitate was filtered off and washed with cold methanol and diethyl ether. Yield: 3.7 g, 88%. Anal. Calcd for $C_{15}H_{18}ClCuN_3O_5$ (419.32): C, 43.0; H, 4.3; N, 10.0. Found: C, 42.8; H, 4.2; N, 9.8. IR (ATR): 3294m, 3243m, 3165w, 1635s, 1605s, 1533m, 1469m, 1453m, 1445m, 1398w, 1353w, 1326 m, 1223w, 1198w, 1150w, 1080s, 1064s, 1044m, 911m, 854w, 758m, 690m, 620m cm^{-1}.

$[(L^1Cu)_3OH](ClO_4)_2$. Addition of an excess of triethylamine to a stirred solution of $[L^1CuPy](ClO_4)$ (0.40 g, 1×10^{-2} mol) in methanol (10 mL) gave a green precipitate that was filtered off 30 min later and washed with cold methanol and diethyl ether. Yield: 0.18 g, 37%. Anal. Calcd for $C_{30}H_{40}Cl_2Cu_3N_6O_{12}$ (938.22): C, 38.4; H, 4.3; N, 9.0. Found: C, 38.1; H, 4.1; N, 8.8. IR (ATR): 3328m, 3264m, 2974w, 1632s, 1602m, 1587m, 1541m, 1468m, 1445s, 1400w, 1302m, 1195m, 1152w, 1118m, 1071s, 1030m, 905m, 849w, 768m, 761m, 658w, 619m cm^{-1}.

$\{[(LCu)_2Ni(CN)_4]\}_n$ ***1.*** A solution of $K_2Ni(CN)_4$ (0.05 g, 0.207 mmol) dissolved in water (2 mL) was added at room temperature to a stirred solution of $[(LCu)_3OH](ClO_4)_2$ (0.13 g, 0.14 mmol) in methanol (10 mL). The resulting solution was filtered 15 min later and kept undisturbed to yield crystals that were isolated by filtration and dried. Yield: 0.07 g, 55%. Anal. Calcd for $C_{22}H_{22}Cu_2N_{10}NiO_2$ (616.2): C, 42.9; H, 3.6; N, 18.2. Found: C, 42.7; H, 3.5; N, 18.0. IR (ATR): 3242m, 3155m, 2170m, 2146s, 1642s, 1597s, 1529m, 1464m, 1449s, 1399m, 1348m, 1320m, 1190m, 1144m, 1121m, 1055m, 1025m, 968m, 927w, 891m, 852w, 753m, 739m, 720w, 638w cm^{-1}.

$[(L^1Cu)_2Ni(CN)_4]$ ***2.*** This compound was prepared in the same way as above with use of $K_2Ni(CN)_4$ (0.065 g, 0.27 mmol) and $[(L^1Cu)_3OH](ClO_4)_2$ (0.17 g, 0.18 mmol). Yield: 0.12 g, 69%. Anal. Calcd for $C_{24}H_{26}Cu_2N_8NiO_2$ (644.3): C, 44.7; H, 4.1; N, 17.4. Found: C, 44.6; H, 3.9; N, 17.2. IR (ATR): 3259m, 3221m, 3142m, 2967w, 2163s, 2129s, 1639s, 1587m, 1532m, 1466m, 1446s, 1377w, 1346m, 1320m, 1298w, 1248w, 1199m, 1147m, 1116m, 1079m, 1053w, 1027w, 907m, 849w, 775m, 693w, 657w, 612w cm^{-1}.

$[LCuAg(CN)_2](MeOH)_2$ ***3.*** Addition of $KAg(CN)_2$ (0.067 g, 0.33 mmol) to a stirred solution of $[(LCu)_3OH](ClO_4)_2$ (0.1 g, 0.11 mmol) in methanol (10 mL) gave a blue solution that was filtered 20 min later and kept undisturbed to yield crystals that were isolated by filtration and dried. Yield: 0.09 g, 67%. Anal. Calcd for $C_{13}H_{19}AgCuN_4O_3$ (450.7): C, 34.6; H, 4.2; N, 12.4. Found: C, 34.3; H, 4.0; N, 12.2. IR (ATR): 3322s, 3264s, 2175m, 2132m, 1644s, 1598m, 1580m, 1537m, 1471m, 1447m, 1395m, 1345m, 1311m, 1196m, 1153m, 1128m, 1099w, 1049m, 1032m, 1007m, 923w, 890w, 856w, 789w, 763m, 750m, 741m, 648m, 634m cm^{-1}.

$\{(L^1CuMeOH)(L^1Cu)[Ag(CN)_2]_2\}(MeOH)_3$ ***4.*** Addition of $KAg(CN)_2$ (0.1 g, 0.48 mmol) to a stirred solution of $[(L^1Cu)_3OH](ClO_4)_2$ (0.15 g, 0.16 mmol) in methanol (10 mL) gave a blue solution that was filtered 20 min later. Slow diffusion of diethyl ether yielded crystals that were isolated by filtration and dried. Yield: 0.12 g, 53%. Anal.

Table 1. Crystallographic Data for Complexes 1−4

	1	2	3	4
formula	$C_{44}H_{44}Cu_4N_{16}Ni_2O_8$	$C_{24}H_{26}Cu_2N_8NiO_2$	$C_{13}H_{19}AgCuN_4O_3$	$C_{28}H_{42}Ag_2Cu_2N_8O_6$
fw	1296.53	644.32	450.73	929.52
space group	$P2_1/n$ (no. 14)	$P\bar{1}$ (no. 2)	*Pbca* (no. 61)	$P2_1/n$ (no. 14)
a, Å	7.4181(18)	6.9732(12)	6.8371(3)	13.6323(4)
b, Å	13.345(3)	7.7262(14)	17.1234(7)	13.8521(4)
c, Å	13.526(3)	11.9453(18)	29.0604(12)	19.2155(5)
α, deg	90	80.228(14)	90	90
β, deg	100.446(4)	82.644(13)	90	96.651(2)
γ, deg	90	89.461(14)	90	90
V, $Å^{-3}$	1316.8(6)	628.96(18)	3402.2(2)	3604.16(18)
Z	1	1	8	4
ρ_{calcd}, g cm^3	1.635	1.701	1.76	1.71
λ, Å	0.71073	0.71073	0.71073	0.71073
T, K	293(2)	180(2)	180(2)	180(2)
μ (Mo K*α*), mm^{-1}	2.352	2.455	2.417	2.284
$R_{obs,\ all}$ [a]	0.0441,0.0549	0.0484, 0.0824	0.0285, 0.0614	0.0453, 0.0751
$R_{wobs,\ all}$ [b]	0.1093, 0.1142	0.1099, 0.1676	0.0301, 0.0463	0.0501, 0.0674

[a] $R = \Sigma||F_o| - |F_c||/\Sigma|F_o|$. [b] $wR_2 = [\Sigma w(|F_o^2| - |F_c^2|)^2/\Sigma w|F_o^2|^2]^{1/2}$.

dx.doi.org/10.1021/ic202157q | *Inorg. Chem.* 2012, 51, 1011−1019

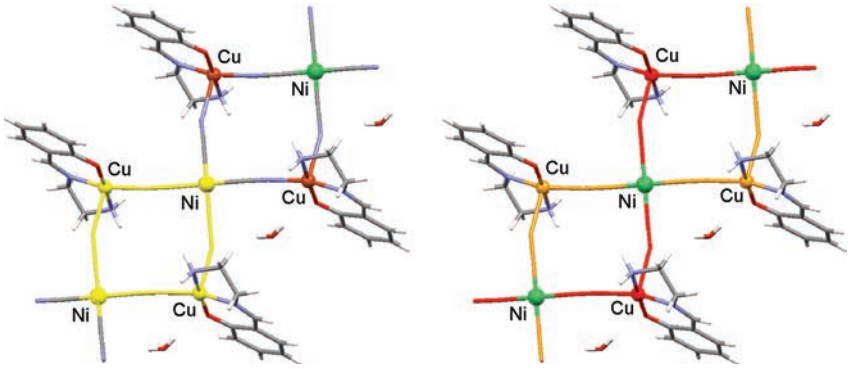

Figure 2. Cu−Ni 1D arrangement in complex **1** viewed as (a) Ni-vertex-shared $[(LCu)_2Ni(CN)_4]$ entities (left) or (b) Cu−Ni alternating intercrossed zigzag chains (right).

Calcd for $C_{28}H_{42}Ag_2Cu_2N_8O_6$ (929.5): C, 36.2; H, 4.6; N, 12.1. Found: C, 36.0; H, 4.6; N, 11.9. IR (ATR): 3326s, 2921w, 2175m, 2137m, 1650s, 1600m, 1537m, 1468m, 1442m, 1394w, 1376w, 1339m, 1306m, 1195m, 1153m, 1129w, 1105w, 1056m, 1032w, 1004m, 904m, 848w, 786w, 764m, 644m cm^{-1}.

Physical Measurements. Elemental analyses were carried out at the Laboratoire de Chimie de Coordination Microanalytical Laboratory in Toulouse, France, for C, H, and N. IR spectra were recorded on a Spectrum 100 FT-IR Perkin-Elmer spectrophotometer using the ATR mode. Magnetic data were obtained with a Quantum Design MPMS SQUID susceptometer. Magnetic susceptibility measurements were performed in the 2−300 K temperature range in a 0.1 T applied magnetic field, and diamagnetic corrections were applied using Pascal's constants.[6] Isothermal magnetization measurements were performed up to 5 T at 2 K. Magnetic susceptibilities have been computed by exact calculations of the energy levels associated to the spin Hamiltonian through diagonalization of the full matrix with a general program for axial and rhombic symmetries[7] and the magnetizations with the MAGPACK program package.[8] Least-squares fittings were accomplished with an adapted version of the function-minimization program MINUIT.[9]

Crystallographic Data Collection and Structure Determination for 1−4. Crystals of **1**−**4** were kept in the mother liquor until they were dipped into oil. The chosen crystals were mounted on a Mitegen micromount and quickly cooled to 180 K. The selected green or blue crystals of **1**−**4** (0.32 × 0.24 × 0.17 (**1**), 0.15 × 0.1 × 0.02 mm^3 (**2**), 0.2 × 0.25 × 0.25 mm^3 (**3**), and 0.15 × 0.2 × 0.35 mm^3 (**4**)) were mounted on an Oxford Diffraction XcaliburBruker (**1** and **2**) or a Kappa APEX II diffractometer (**3** and **4**) using graphite-monochromated Mo Kα radiation (λ = 0.71073 Å) and equipped with an Oxford Cryosystems Cryostream Cooler Device. Data were collected at low temperature (180 K), except for **1**, at 293 K, Table 1. The final unit cell parameters have been obtained by means of least-squares refinements. The structures have been solved by direct methods using SIR92[10] and refined by means of least-squares procedures on F^2 with the program SHELXL97[11] included in the software package WinGX version 1.63[12] for complexes **1** and **2**, while refinements were carried out by full-matrix least-squares on F with CRYSTALS[13] for complexes **3** and **4**. The atomic scattering factors were taken from the *International Tables for X-ray Crystallography*.[14] All non-hydrogen atoms were anisotropically refined, and in the last cycles of refinement a weighting scheme was used, where weights were calculated with the following formula: $w = 1/[\sigma^2(F_o^2) + (aP)^2 + bP]$, where $P = (F_o^2 + 2F_c^2)/3$.

Computational Details. All theoretical calculations were carried out at the DFT level of theory using the hybrid B3LYP exchange-correlation functional,[15] as implemented in the Gaussian 03 program.[16] A quadratic convergence method was employed in the SCF process.[17] The triple-ζ quality basis set proposed by Ahlrichs and co-workers has been used for all atoms.[18] Calculations were performed on the complexes built from the experimental geometries as well as on model complexes. The electronic configurations used as starting points were created using Jaguar 7.7 software.[19] The approach used to determine the exchange coupling constants for polynuclear complexes has been described in detail elsewhere.[20]

RESULTS

Reaction of cationic copper complexes, namely, $[LCuPy]^+$, $[(LCu)_3OH]^{2+}$, and $[(L^1Cu)_3OH]^{2+}$, with diverse polycyanometallate tectons yielded neutral entities whatever the tecton used, $[Ni(CN)_4]^{2-}$ (structures **1** and **2**) or $[Ag(CN)_2]^-$ (structures **3** and **4**). To date, we found in the literature only a unique paper reporting the reaction of $[Fe(CN)_6]^{3-}$ with a copper complex resulting in complexation of a tridentate ligand which allows formation of a polymetallic complex through the remaining equatorial position.[21] The ligand used in that reference possesses a terminal tertiary amine function instead of a primary amine function as in the present work, a change that induces formation of quite different structures for the resulting complexes. The IR spectra show two sharp peaks in the CN stretching region, which are consistent with either the presence of terminal and bridging cyano groups or the existence of different bridging modes. Use of two different starting copper complexes, one made with an achiral tridentate unit and the other one with the racemic form of an asymmetric ligand, will be helpful to understand the intricate magnetic behavior of some of these complexes. This point is developed in the following section.

Structural Determinations. X-ray diffraction analyses have been made for complexes **1**−**4**. Complex $\{[(LCu)_2Ni(CN)_4]\}_n$ (**1**) crystallizes in the monoclinic $P2_1/n$ space group (with Z = 1). The structure scaffold is based on square-planar $Ni(CN)_4^{2-}$ tectons connecting two LCu^+ units, giving rise to formation of a 1D chain constituted by Ni-vertex-sharing $[(LCu)_2Ni(CN)_4]$ entities, see Figure 2. This chain can also be analyzed as resulting from the assembling of two Cu−Ni alternating zigzag chains crossing at each Ni atom position (Figure 2). In the structure, the four cyano nitrogen atoms are involved in the coordination bonding with copper ions in such a manner that each copper atom is pentacoordinated and linked to two (axial + equatorial) cyano functions. As a result, each pair of trans cyano groups belonging to a $Ni(CN)_4^{2-}$ species alternatively connects two LCu units through axial and equatorial positions.

There is a water molecule per $[(LCu)_2Ni(CN)_4]$ unit, which is hydrogen bonded to the phenoxo oxygen atom of a ligand and to the primary amine of a neighboring unit following a O···H_2O···H_2N scheme. Therefore, each LCu unit ends up being linked to two different chains. As expected, the Cu···Cu distances through the NC−Ni—CN bridge are shorter for

dx.doi.org/10.1021/ic202157q | *Inorg. Chem.* 2012, 51, 1011−1019

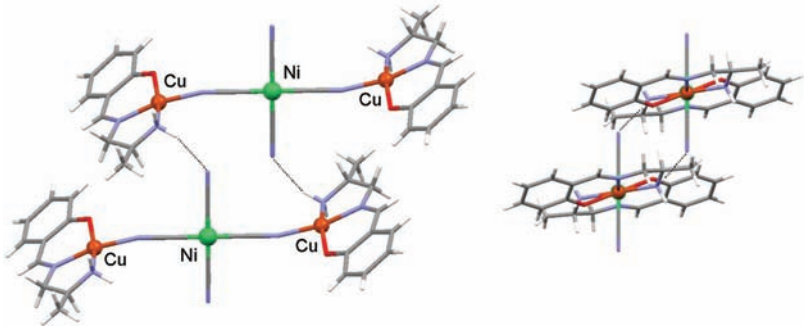

Figure 3. Different views of the molecular structure of complex **2**: (a) front view (left) and (b) side view along the CuNiCu axis (right).

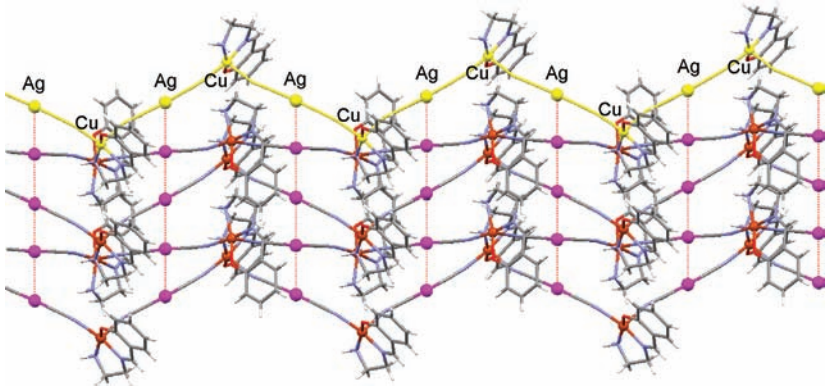

Figure 4. Structure of complex **3**. Straight horizontal lines represent the chains turned by 67° with respect to the yellow-marked reference.

equatorially bridged copper ions (9.957(2) Å) than for those bridged through their axial positions (10.645(2) Å). The interchain distance measured through the above-mentioned hydrogen-bond bridge is equal to 8.030(2) Å.

Complex $[(L^1Cu)_2Ni(CN)_4]$ (**2**) crystallizes in the triclinic *P*-1 space group (with $Z = 1$). In this structure, two L^1Cu^+ cationic entities are linked, through their equatorial plane, to two trans cyano groups of the $Ni(CN)_4^{2-}$ tecton in a head-to-tail arrangement, the Ni^{II} atom being located in a center of symmetry (Figure 3). The copper(II) ion possesses a square planar N_3O environment: the oxygen and two nitrogen atoms coming from the half-unit L^1 ligand, the last nitrogen atom from a cyano function. There are no geometrical isomers, the asymmetric carbon atom being only in the remote position compared to the imine bond.[22] As we start with racemic L^1Cu species, a *Sδ* stereoisomer is associated with a *Rλ* one in each $[(L^1Cu)_2Ni(CN)_4]$ unit. These stereoisomers depend on the chirality (*R* or *S*) of the substituted carbon atom (Figure 3) and on the conformation (*δ* or *λ*) of the metallo-imidazolidine five-membered ring. The two uncoordinated cyano groups are involved in hydrogen bonds with the primary amine functions of proximal L^1Cu moieties, thus yielding an infinite chain in which the $[(L^1Cu)_2Ni(CN)_4]$ units are held together by a couple of complementary and centrosymmetrically related N···H_2N hydrogen bonds. The Cu···Cu distance through the NC−Ni—CN bridge is equal to 9.831(2) Å, while the Cu···Cu distance between two different $[(L^1Cu)_2Ni(CN)_4]$ units (wich are made of identical stereoisomers, *Sδ* or *Rλ*) are separated by 6.973(1) Å.

The crystal structure of complex **3** consists of neutral $[(LCu)Ag(CN)_2]$ entities and two crystallization methanol molecules giving rise to a 2D scaffold consisting of two differently oriented noninterlaced zigzag Cu−Ag chains that crystallize in the orthorhombic *Pbca* space group (with $Z = 8$), where the copper centers are also pentacoordinated. The two planes defining each chain orientation are turned by 67.0° (Figure S1, Supporting Information). The structure of each chain (marked in yellow in Figure 4) does not differ very much from that of the zigzag chains represented for complex **1** (Figure 2, right). In fact, the Cu−O and Cu−N bond lengths as well as the distances inside the ligand do not significantly vary from those observed for this complex. In **3**, however, the $[(LCu)Ag(CN)_2]$ units within the chain are connected following an alternating axial−equatorial coordination scheme for the cyano groups directly attached to the copper(II) ions. The 2D structure, see Figure 4, is acquired by establishment of interchain argentophilic interactions, with a Ag−Ag distance of 3.4217(6) Å, within the typical range established for such interactions (between 2.963 and 3.655 Å).[23]

Two consecutive chains belonging to parallel planes are separated by 6.8371(7) Å (measured from the Ag−Ag distance), while the Cu···Cu distance through the NC−Ag—CN bridge is equal to 10.5563(5) Å. At the same time, for two proximal differently oriented chains, a Cu···Cu distance of 6.1801(5) Å is observed. Two-type methanol molecules are located along the Ag positions and participate in the structure by establishment of several interactions: one type is hydrogen bonded both to the phenoxo oxygen atom of each LCu unit and to the second type methanol molecules, and the second type are interacting with the Ag atoms through purely electrostatic Ag−O interactions at 2.865(3) Å.

The 1D structure of **4** consists of trinuclear cationic $\{[L^1Cu(MeOH)][Ag(CN)_2](L^1Cu)\}^+$ entities, $[Ag(CN_2)]^-$ anions, and three methanol molecules (Figure 5) and crystallizes in the monoclinic $P2_1/n$ space group (with $Z = 4$). Within the cationic Cu_2Ag units, two square-pyramidal

dx.doi.org/10.1021/ic202157q | *Inorg. Chem.* 2012, 51, 1011−1019

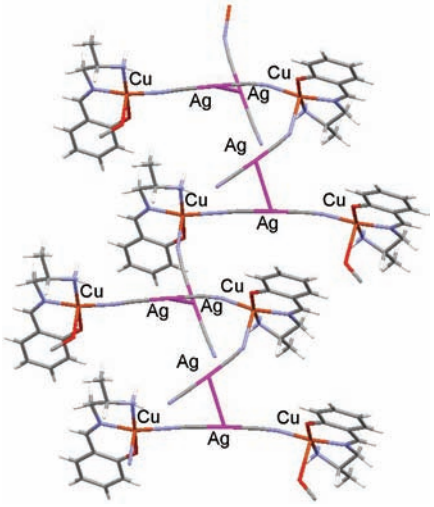

Figure 5. 1D structure of complex **4** through argentophilic interactions.

pentacoordinated L^1Cu units are equatorially connected by the NC−Ag−CN bridge, as in complex **2**, with a Cu···Cu distance of 10.1614(7) Å. One of the L^1Cu units saturates the apical coordination position with a methanol molecule, whereas the copper(II) ion of the other L^1Cu unit completes its coordination sphere with the nitrogen atom of a monocoordinated $[Ag(CN_2)]^-$ anion. This monocoordinated $[Ag(CN_2)]^-$ is linked by one of its nitrogen atoms to a methanol molecule. The bridged and monocoordinated $[Ag(CN_2)]^-$ entities exhibit argentophilic interactions with a Ag−Ag separation of 3.0563(5) Å, which is significantly shorter than that observed in complex **3**, ultimately leading to a chain. Contrary to complex **2**, the $[Ag(CN_2)]^-$ anion bridges two *Sδ* stereoisomers while a neighbor $[Ag(CN_2)]^-$ moiety, belonging to another cationic Cu_2Ag entity, bridges two *Rλ* stereoisomers.

Along the chain arrangement, the separation between intrachain L^1Cu units, which are not directly coordinated, alternately varies between 8.1587(7) and 8.4262(7) Å. Two of these chains interact between themselves by two O(phenoxo)···HOMe hydrogen bonds that yield very short Cu···Cu interchain distances (5.0113(6) Å), while additional NH_2···MeOH···MeOH···O(phenoxo) hydrogen bonds involve the primary amine functions with the two remaining methanol molecules and the phenoxo oxygen atom linked to the Cu ion bearing the NC cyano group in the axial position.

Magnetic Properties. From the magnetic point of view, the simplest example is given by complex **2**; thus, it is studied first. The $\chi_M T$ product reported in Figure 6 is equal to 0.80 cm^3 mol^{-1} K at 300 K (as expected for two isolated Cu^{II} ions) and remains constant until 15 K before decreasing to 0.56 cm^3 mol^{-1} K at 2 K. As mentioned above, the experimental data indicate the occurrence of an overall weak antiferromagnetic interaction in **2**. The best fit of the magnetic data with the isotropic Hamiltonian $H = -2J_{CuCu}(S_{Cu1}\cdot S_{Cu2})$ gives the following parameters: $J_{CuCu} = -0.75$ cm^{-1}, $g = 2.08$, and $R = 8.0 \times 10^{-5}$, with $R = \Sigma[(\chi_M T)^{obs} - (\chi_M T)^{calcd}]^2/\Sigma(\chi_M T)^{obs}]^2$.

For complex **1**, the $\chi_M T$ product is constant from 300 (0.85 cm^3 mol^{-1} K) to approximately 10 K (0.86 cm^3 mol^{-1} K) and then increases to 0.93 cm^3 mol^{-1} K at 2 K; this behavior corresponds to a global weak ferromagnetic coupling. The participation of the four bridging cyano groups of the $[Ni(CN)_4]^{2-}$ tecton creates two intercrossed 1D zigzag chains

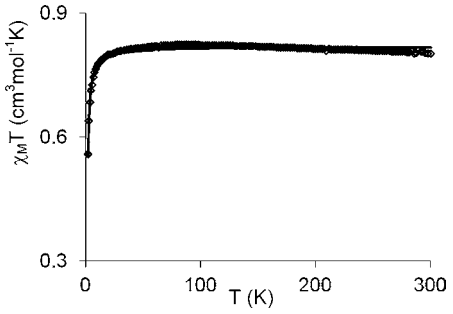

Figure 6. Temperature dependence of the $\chi_M T$ product for complex **2**. Solid line corresponds to the best data fit (see the text).

in which the Ni^{II} ion is linked to two trans Cu^{II} ions through equatorial positions in one chain and to two trans Cu^{II} ions through axial positions in the other chain. Thus, if we suppose that the axial−axial bridging pathway is noneffective (since the unpaired electron is placed in the d_{x2-y2} orbital directed toward the equatorial positions), the double chain can be reduced to dinuclear Cu−Cu units equatorially connected by a $Ni(CN)_2$ unit. A fitting with the isotropic Hamiltonian $H = -2J_{CuCu}(S_{Cu1}\cdot S_{Cu2})$ gives $J = +0.30$ cm^{-1}, $g = 2.12$, and $R = 3 \times 10^{-5}$ (Figure S2, Supporting Information). This result is surprising if we remember that complex **2**, which is a true dinuclear species with equatorial bridges, is governed by weak antiferromagnetic interactions. Such an observation means that the retained model for complex **1** is wrong. A trial with an approximate model taking into account four copper ions, one equatorial-equatorial J and four *cis* equatorial-axial J' interactions (the axial−axial J'' interactions was assumed to be negligible) using the Hamiltonian $H = -2J_{CuCu}(S_{Cu1}\cdot S_{Cu2}) - 2J'_{CuCu}(S_{Cu1}\cdot S_{Cu3} + S_{Cu3}\cdot S_{Cu2} + S_{Cu2}\cdot S_{Cu4} + S_{Cu4}\cdot S_{Cu1})$ gives a more realistic solution (Figure 7) with $J = -0.37$ cm^{-1}, $J' = +0.32$ cm^{-1}, $g = 2.08$, and R

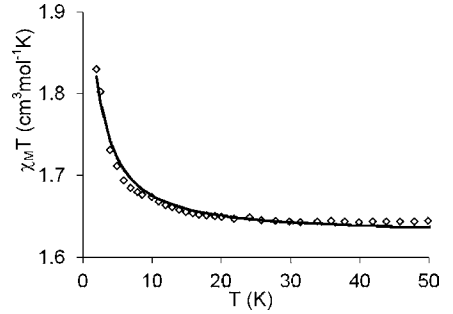

Figure 7. Temperature dependence of the $\chi_M T$ product for complex **1**. Solid line corresponds to the best data fit (see the text).

$= 1 \times 10^{-4}$ (see later Figure 10 for a better understanding of the possible magnetic exchange interactions).

We take into account that the retained model does not correspond to the real situation. If the model is correct for the equatorial−equatorial J Cu−Cu interaction, it overestimates the axial−equatorial J' Cu−Cu interaction.

In the case of complex **3**, a different magnetic behavior is observed (Figure 8). The $\chi_M T$ product is constant from 300 (0.89 cm^3 mol^{-1} K) to approximately 10 K (0.91 cm^3 mol^{-1} K) and then increases to 0.99 cm^3 mol^{-1} K at 2 K, which corresponds to a global weak ferromagnetic behavior. The structural data show that complex **3** corresponds to a 1D zigzag chain in which two copper ions are bridged through a NC−

dx.doi.org/10.1021/ic202157q | Inorg. Chem. 2012, 51, 1011−1019

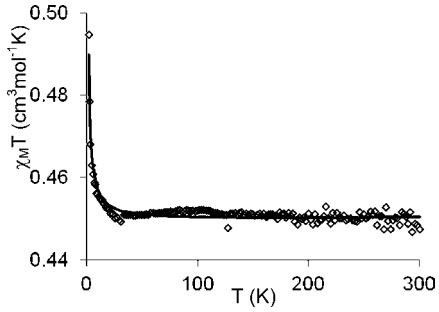

Figure 8. Temperature dependence of the $\chi_M T$ product for complex **3**. Solid line corresponds to the best data fit (see the text).

Ag−CN unit through axial and equatorial positions alternately. A fit using a chain model furnishes a J parameter equal to +0.10 cm^{-1} with $g = 2.19$ and $R = 1.0 \times 10^{-4}$ (Figure 8). The positive J value is easily explained by the orthogonality of the involved copper magnetic orbitals. We remark that a fit using the isotropic Hamiltonian $H = -2J_{CuCu}$ $(S_{Cu1} \cdot S_{Cu2})$ gives a J parameter of +0.25 cm^{-1} with $g = 2.19$ and $R = 1.0 \times 10^{-4}$, overestimated by a 2.5 factor in comparison to the chain model (Figure S3, Supporting Information).

A similar behavior, with respect to complex **2**, was found for complex **4** (Figure 9). The experimental $\chi_M T$ product is equal

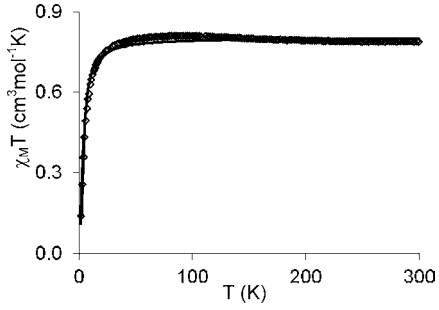

Figure 9. Temperature dependence of the $\chi_M T$ product for complex **4**. Solid line corresponds to the best data fit (see the text).

to 0.79 cm^3 mol^{-1} K at 300 K and remains constant until 40 K, where it starts to decrease smoothly until 10 K (0.63 cm^3 mol^{-1} K) and then more abruptly to 0.14 cm^3 mol^{-1} K at 2 K. The best fit gives $J_{CuCu} = -2.23$ cm^{-1}, $g = 2.07$, and $R = 7.0 \times 10^{-4}$.

DFT Calculations. We also performed DFT calculations in order to support the experimental data obtained for these complexes and evaluate the effects of (i) the actual magnitude of the magnetic coupling between the copper(II) ions through the diamagnetic center and (ii) the different magnetic coupling in function of the spatial disposition of the copper centers, namely, axial−axial, axial−equatorial, and equatorial−equatorial. In principle, axial−axial magnetic coupling is expected to be negligible because the spin density of the copper(II) unpaired electrons is not located along this direction (the magnetic orbital of the copper(II) ion is of the d_{x2-y2} type and directed toward the donor atoms in the basal plane of the copper(II) square pyramidal coordination sphere). On the other hand, the axial−equatorial magnetic interaction should be ferromagnetic because the involved orbitals are mutually orthogonal. The equatorial-equatorial pathway, however, should lead to an antiferromagnetic interaction. It should be noted that we just calculated the theoretical J values for complexes **1** and **2**, because we did not have available all-electron basis sets for silver. Use of pseudopotentials for this metallic center did not offer the reliable results we need with respect to the extremely accurate, all-purpose B3LYP/TZV functional/basis set combination.[15]

For complex **1**, we considered the fragment **1-calc** formed by a square of copper ions surrounding a chain of three diamagnetic Ni^{II} ions connecting the copper centers by cyano bridges, see Figure 10. This fragment allows us to consider all

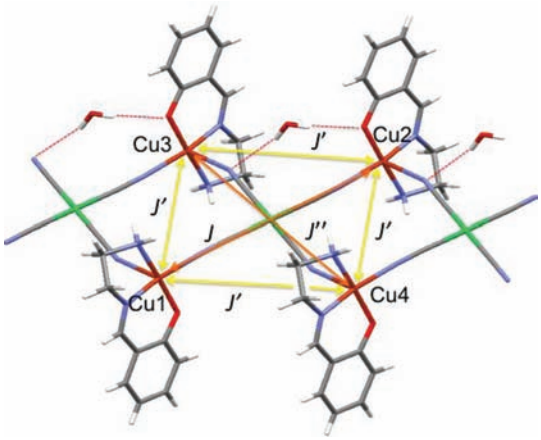

Figure 10. 1-calc structure showing the different calculated pathways.

the interactions needed for accurately solving the square moiety: a six-J system formed by the four sides and the two diagonals of the copper square. However, from the calculations, all J values corresponding to the sides (J') are equal between them and ferromagnetic, +0.01 cm^{-1}, as expected as they correspond to axial−equatorial interactions (orthogonal orbitals). The J value corresponding to the axial−axial pathway diagonal (J'') is exactly zero, as expected for zero-delocalized spin density pathways. The other diagonal pathway, J, corresponding to an equatorial−equatorial interaction, gave a value of −0.31 cm^{-1}, in perfect agreement with the expected values. The zero value obtained for the axial−axial pathway indicates that even in the cases where the J values are very low DFT calculations are reliable.

In order to evaluate the magnetic interdependence existing between the different pathways we decomposed the calculated structure **1-calc** in three parts to get the axial−axial (**1-calc**$_{ax}$), axial−equatorial (**1-calc**$_{ax\text{-}eq}$), and equatorial−equatorial (**1-calc**$_{eq}$) interactions separately, see Figure 11.

From these calculations, we obtained the following results, thus confirming the previous values: $J_{ax} = 0$ cm^{-1}, $J_{ax-eq} = +0.02$ cm^{-1}, and $J_{eq} = -0.35$ cm^{-1}.

For complex **2**, however, we considered the whole copper dimer, which exhibits an equatorial−equatorial magnetic pathway between the copper ions (see Figure 12, left). Therefore, an antiferromagnetic coupling would be expected for the Cu−Cu magnetic interaction. In good agreement, DFT calculations showed a J value of −0.35 cm^{-1}, exactly the same value as that obtained for the decomposed equatorial−equatorial **1-calc**$_{eq}$ structure previously calculated.

Moreover and with the aim to validate our calculations, we selected another additional structure to be calculated: the bibliographic closely related VATCEZ structure,[24] for which only axial−axial magnetic interactions are operative between the copper(II) ions (Figure 12, right). For this structure we obtained, as expected, a strictly zero J value.

dx.doi.org/10.1021/ic202157q | Inorg. Chem. 2012, 51, 1011−1019

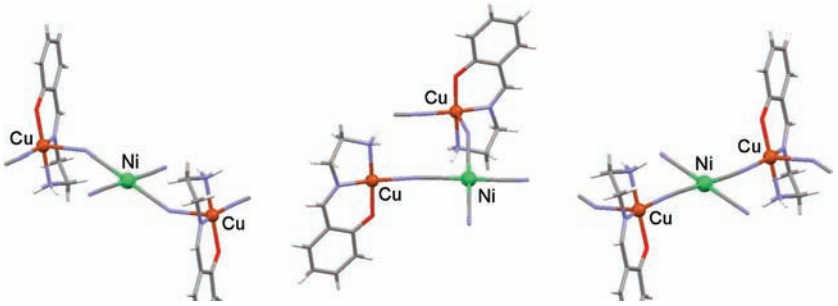

Figure 11. Decomposition of the calculated **1-calc** structure for independent evaluation of the different pathways.

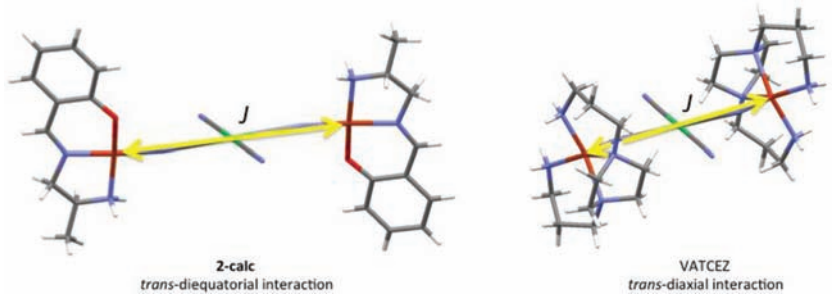

Figure 12. Calculated **2-calc** structure (left), and the related diaxial structure VATCEZ (right).

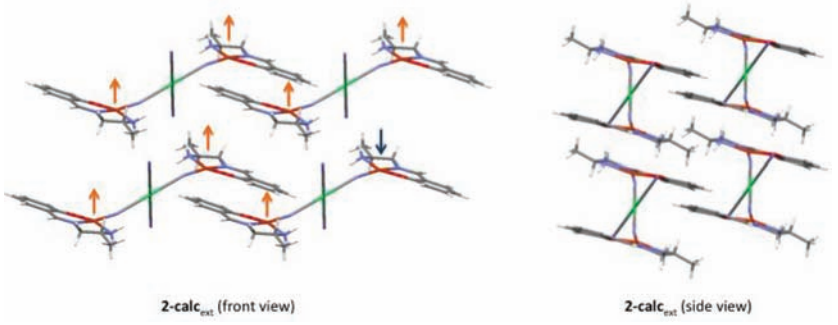

Figure 13. Two views of the considered extended system **2-calc$_{ext}$** showing the spin distribution for evaluation of J^1 with respect to the high-spin (S = 4) situation (left).

The relatively small size of complex **2-calc** allowed us to calculate an extended system consisting of four proximal copper dimers (Figure 13). The system is now, however, too big to calculate the high number of possible magnetic interactions between all the centers. We can, nevertheless, make an approach to reduce the number of calculated states. This strategy allows us to get a new 'global' J^1 value for this system. The term 'global' refers here to the fact that some intermolecular interactions are also taken into account in such a manner that J^1 (which could be considered as an approximation to the sum $J + J_{inter}$), in principle, would offer a closer value to the experimental one, which globally considers all the interactions involved along the crystal. In this case, the displayed intermolecular interactions affect the uncoordinated cyano groups to the copper atoms, which experiences some influence of the hydrogen atoms of the amino groups of the ligand. Thus, taking one of the inner copper dimers as reference for our calculations, see Figure 13, we determined that J^1 = −0.42 cm^{-1}, which means that the intermolecular interactions are AF in nature, although very small ($J_{inter} \approx -0.07$ cm^{-1}).

CONCLUSIONS

The study of magnetic interactions in polynuclear complexes mainly focuses on the nearest-neighbor interactions, but in presence of more than two active centers, the next-nearest-neighbor interactions, which are not easy to evidence from an experimental point of view, have to be taken into account. The aim of the present work consisted in the study of long-range magnetic interaction established by different pathways through diamagnetic metallic centers, which explains the voluntary presence of a diamagnetic metal ion (Ni^{II}, Ag^{I}) in between the magnetically active copper centers in the four examples studied here. This also explains the choice of polycyanometallate tectons that easily bridge two metal ions leading them to a distance of about 10 Å. Use of an asymmetric copper−ligand entity has led to different species that have greatly facilitated the understanding of the magnetic behavior. Indeed, a first look at the magnetic behavior of complex **1** is puzzling. A global ferromagnetic interaction is evidenced when the structural determination indicates that the main interaction involves two copper ions bridged in their equatorial positions, a situation that should favor an overlap of the active d_{x2-y2} copper orbitals located in the basal plane, yielding to an antiferromagnetic

dx.doi.org/10.1021/ic202157q | Inorg. Chem. 2012, 51, 1011−1019

interaction. Owing to the complexation of two different enantiomers (*R* and *S*) in a trans disposition of a NC−Ni−CN bridge for complex **2**, the 1D arrangement found in complex **1** is no longer possible. Complex **2** behaves as a well-isolated dinuclear species, and we can confirm that the equatorial−equatorial Cu−Cu arrangement does give a weak antiferromagnetic interaction (−0.75 cm^{-1}) as expected. If we do not take into consideration the argentophilic Ag−Ag interaction, a similar situation happens in complex **4**, the difference being that two *R* or two *S* enantiomers are now bridged through the same NC−Ag−CN bridge. The antiferromagnetic interaction becomes larger, −2.23 cm^{-1} instead of −0.75 cm^{-1}, as a consequence of the more diffuse Ag orbitals intervening through the bridge, in comparison to the Ni orbitals. The different charges present in both metals also can affect the coupling. Complex **3** is quite informative as the NC−Ag−CN unit bridges two LCu entities in equatorial and axial positions, introducing orthogonality of the magnetic copper orbitals and, by consequence, a ferromagnetic J_{CuCu} interaction. In our complex the trans arrangement of the LCu entities yields a ferromagnetic *J* value varying from 0.10 to 0.25 cm^{-1}, depending on the retained model (chain or dinuclear species). We can imagine that a cis arrangement must also give a ferromagnetic interaction. Keeping these results in mind and reducing the 1D chain for **1** to four LCu units linked to the four nitrogen atoms of the diamagnetic $Ni(CN)_4$ bridging unit, complex **1** involves four ferromagnetic cis axial−equatorial Cu−Cu interactions, one antiferromagnetic equatorial−equatorial, and one axial−axial interaction supposed to be null. Such a model gives a satisfactory fit with *J* values of +0.32 and −0.37 cm^{-1}, respectively. As we previously underlined that the axial−equatorial Cu−Cu interactions are overestimated in our model and in agreement with the different *J* values found for complex **3**, an upper limit of 0.13 cm^{-1} for *J*′ seems to be more appropriate.

Finally, ad hoc DFT calculations showed that actually there is a small transmission of the magnetic effect through the diamagnetic metallic bridge. Additionally, these calculations establish that the different magnetic pathways, based on a different orientation of the involved magnetic orbitals, are almost independent between them, observing a strictly zero *J* value for zero-delocalized spin density pathways (axial−axial interactions), a ferromagnetic behavior for orthogonal interacting orbitals (axial−equatorial interactions), and an antiferromagnetic magnetic interaction for direct-interacting orbitals (equatorial−equatorial interactions).

■ ASSOCIATED CONTENT

Ⓢ Supporting Information

This material is available free of charge via the Internet at http://pubs.acs.org.

■ AUTHOR INFORMATION

Corresponding Author

*E-mail: costes@lcc-toulouse.fr.

■ ACKNOWLEDGMENTS

We thank the MEC (Spain) (Project CTQ-2008-02269/BQU), the Junta de Andalucía (FQM-195 and Project of excellence FQM-3705), and the University of Granada. We also thank the Centro de Supercomputación de la Universidad de Granada (UGRGRID) for computational resources. The authors are also grateful to Dr. José A. Gavira, from the laboratory for crystallographic studies, CSIC, Granada, for his generous assistance with X-ray data collection of compound **1**.

■ REFERENCES

(1) (a) Dunbar, K. R.; Heintz, R. A. *Prog. Inorg. Chem.* **1996**, *45*, 283−391. (b) Verdaguer, M.; Bleuzen, A.; Marvaud, V.; Vaissermann, J.; Seuleiman, M.; Desplanches, C.; Scuiller, A.; Train, C.; Garde, R.; Gelly, G.; Lomenech, C.; Rosenman, I.; Veillet, P.; Cartier, C.; Villain, F. *Coord. Chem. Rev.* **1999**, *190−192*, 1023−1047. (c) Ohba, M.; Okawa, H. *Coord. Chem. Rev.* **2000**, *198*, 313−328. (d) Cernak, J.; Orendac, M.; Potocnak, I.; Chomic, J.; Orendacova, A.; Skorsepa, J.; Feher, A. *Coord. Chem. Rev.* **2002**, *224*, 51−66. (e) Przychodzen, P.; Korzeniak, T.; Podgajny, R.; Sieklucka, B. *Coord. Chem. Rev.* **2006**, *250*, 2234−2260.

(2) Lescouëzec, R.; Toma, L. M.; Vaissermann, J.; Verdaguer, M.; Delgado, F. S.; Ruiz-Pérez, C.; Lloret, F.; Julve, M. *Coord. Chem. Rev.* **2005**, *249*, 2691−2729.

(3) Marvaud, V.; Decroix, C.; Scuiller, A.; Tuyèras, F.; Guyard-Duhayon, C.; Vaissermann, J.; Marrot, J.; Gonnet, F.; Verdaguer, M. *Chem.—Eur. J.* **2003**, *9*, 1692−1705.

(4) Cros, G.; Costes, J. P. *C. R. Acad. Sci. Paris, Ser II* **1982**, 173−175. (b) Costes, J. P.; Fenton, D. *J. Chem. Soc., Dalton Trans.* **1983**, 2235−2239. (c) Costes, J. P.; Dahan, F.; Laurent, J. P. *Inorg. Chem.* **1986**, *25*, 413−416. (d) Costes, J. P.; Fernandez-Garcia, M. I. *Inorg. Chim. Acta* **1995**, *237*, 57−63.

(5) (a) Costes, J. P. *Bull. Soc. Chim. Fr.* **1986**, 78−82. (b) Costes, J. P.; Dahan, F.; Fernandez-Fernandez, M. B.; Fernandez-Garcia, M. I .; Garcia-Deibe, A. M.; Sanmartin, J. *Inorg. Chim. Acta* **1998**, *274*, 73−81.

(6) Pascal, P. *Ann. Chim. Phys.* **1910**, *19*, 5−70.

(7) Boudalis, A. K.; Clemente-Juan, J.-M.; Dahan, F.; Tuchagues, J.-P. *Inorg. Chem.* **2004**, *43*, 1574−1586.

(8) Borrás-Almenar, J. J.; Clemente-Juan, J. M.; Coronado, E.; Tsukerblat, B. S. *Inorg. Chem.* **1999**, *38*, 6081−6088. Borrás-Almenar, J. J.; Clemente-Juan, J. M.; Coronado, E.; Tsukerblat, B. S. *J. Comput. Chem.* **2001**, *22*, 985−991.

(9) James, F.; Roos, M. *Comput. Phys. Commun.* **1975**, *10*, 343−367.

(10) SIR92-A program forcrystal structure solution. Altomare, A.; Cascarano, G.; Giacovazzo, C.; Guagliardi, A. *J. Appl. Crystallogr.* **1993**, *26*, 343−350.

(11) Sheldrick, G. M. *SHELX97 [Includes SHELXS97, SHELXL97, CIFTAB]-Programs for Crystal Structure Analysis (Release 97-2)*; Institüt für Anorganische Chemie der Universität: Göttingen, Germany, 1998.

(12) WINGX-1.63 IntegratedSystem of Windows Programs for the Solution, Refinement and Analysisof Single Crystal X-Ray Diffraction Data. Farrugia, L. *J. Appl. Crystallogr.* **1999**, *32*, 837−838.

(13) Betteridge, P. W.; Carruthers, J. R.; Cooper, R. I.; Prout, K.; Watkin, D. J. *J. Appl. Crystallogr.* **2003**, *36*, 1487.

(14) *International tables for X-Ray crystallography*; Kynoch Press: Birmingham, England, 1974; Vol. *IV*.

(15) (a) Becke, A. D. *Phys. Rev. A* **1988**, *38*, 3098−3100. (b) Lee, C.; Yang, W.; Parr, R. G. *Phys. Rev. B* **1988**, *37*, 785−789. (c) Becke, A. D. *J. Chem. Phys.* **1993**, *98*, 5648−5652.

(16) Frisch, M. J.; Trucks, G. W.; Schlegel, H. B.; Scuseria, G. E.; Robb, M. A.; Cheeseman, J. R.; Montgomery, Jr., J. A.; Vreven, T.; Kudin, K. N.; Burant, J. C.; Millam, J. M.; Iyengar, S. S.; Tomasi, J.; Barone, V.; Mennucci, B.; Cossi, M.; Scalmani, G.; Rega, N.; Petersson, G. A.; Nakatsuji, H.; Hada, M.; Ehara, M.; Toyota, K.; Fukuda, R.; Hasegawa, J.; Ishida, M.; Nakajima, T.; Honda, Y.; Kitao, O.; Nakai, H.; Klene, M.; Li, X.; Knox, J. E.; Hratchian, H. P.; Cross, J. B.; Adamo, C.; Jaramillo, J.; Gomperts, R.; Stratmann, R. E.; Yazyev, O.; Austin, A. J.; Cammi, R.; Pomelli, C.; Ochterski, J. W.; Ayala, P. Y.; Morokuma, K.; Voth, G. A.; Salvador, P.; Dannenberg, J. J.; Zakrzewski, V. G.; Dapprich, S.; Daniels, A. D.; Strain, M. C.; Farkas, O.; Malick, D. K.; Rabuck, A. D.; Raghavachari, R.; Foresman, J. B.; Ortiz, J. V.; Cui, Q.; Baboul, A. G.; Clifford, S.; Cioslowski, J.; Stefanov, B. B.; Liu, G.; Liashenko, A.; Piskorz, P.; Komaromi, I.; Martin, R. L.; Fox, D. J.; Keith, T.; Al-Laham, M. A.; Peng, C. Y.;

Nanayakkara, A.; Challacombe, M.; Gill, P. M. W.; Johnson, B.; Chen, W.; Wong, M. W.; Gonzalez, C.; Pople, J. A. *Gaussian 03*, Revision E.01; Gaussian, Inc.: Wallingford, CT, 2004.
(17) Bacskay, G. B. *Chem. Phys.* **1981**, *61*, 385−404.
(18) Schaefer, A.; Huber, C.; Ahlrichs, R. *J. Chem. Phys.* **1994**, *100*, 5829−5835.
(19) *Jaguar 7.7*; Schrödinger, Inc.: Portland, OR, 2010.
(20) Ruiz, E.; Cano, J.; Alvarez, S.; Alemany, P. *J. Comput. Chem.* **1999**, *20*, 1391−1400. (b) Ruiz, E.; Alvarez, S.; Rodríguez-Fortea, A.; Alemany, P.; Puoillon, Y.; Massobrio, C. In *Magnetism: Molecules to Materials*; Miller, J. S., Drillon, M., Eds.; Wiley-VCH: Weinheim, 2001; Vol. *II*, p 5572. (c) Ruiz, E.; Alvarez, S.; Cano, J.; Polo, V. *J. Chem. Phys.* **2005**, *123*, 164110−164117.
(21) Maxim, C.; Sorace, L.; Khuntia, P.; Madalan, A. M.; Kravtsov, V.; Lascialfari, A.; Caneschi, A.; Journaux, Y.; Andruh, M. *Dalton Trans.* **2010**, *39*, 4838−4847.
(22) Costes, J. P.; Dahan, F.; Dominguez-Vera, J. M.; Laurent, J. P.; Ruiz, J.; Sotiropoulos, J. *Inorg. Chem.* **1994**, *33*, 3908−3913.
(23) Zhang, J.; Shen, Y.-Ch.; Qin, Y.-Y.; Liab, Zh.-J.; Yao, Y.-G. *CrystEngComm* **2007**, *9*, 636−639.
(24) Smékal, Z.; Trávníček, Z.; Mroziński, J.; Marek, J. *Inorg. Chem. Commun.* **2003**, 1395−1399.